β amyloid protein precursor-like (*Appl*) is a Ras1/MAPK-regulated gene required for axonal targeting in *Drosophila* photoreceptor neurons

Natalia Mora[1], Isabel Almudi[1,*], Berta Alsina[2], Montserrat Corominas[1] and Florenci Serras[1,‡]

[1]Departament de Genètica, Facultat de Biologia, Institut de Biomedicina de la Universitat de Barcelona (IBUB), Universitat de Barcelona, Diagonal 645, 08028 Barcelona, Spain
[2]Department of Experimental and Health Sciences (CEXS), Universitat Pompeu Fabra, Barcelona Biomedical Research Park (PRBB), 08003 Barcelona, Spain

*Present address: Evolution of Animal Development and Morphology, Department of Biological and Medical Sciences, Oxford Brookes University, Oxford, UK
‡Author for correspondence (fserras@ub.edu)

Accepted 4 November 2012
Journal of Cell Science 126, 53–59

doi: 10.1242/jcs.114785

Summary

In a genome-wide expression profile search for genes required for *Drosophila* R7 photoreceptor development we found *β amyloid protein precursor-like* (*Appl*), the ortholog of human *APP*, which is a key factor in the pathogenesis of Alzheimer's disease. We analyzed *Appl* expression in the eye imaginal disc and found that is highly accumulated in R7 photoreceptor cells. The R7 photoreceptor is responsible for UV light detection. To explore the link between high expression of Appl and R7 function, we have analyzed *Appl* null mutants and found reduced preference for UV light, probably because of mistargeted R7 axons. Moreover, axon mistargeting and inappropriate light discrimination are enhanced in combination with neurotactin mutants. R7 differentiation is triggered by the inductive interaction between R8 and R7 precursors, which results in a burst of Ras1/MAPK, activated by the tyrosine kinase receptor Sevenless. Therefore, we examined whether Ras1/MAPK is responsible for the high *Appl* expression. Inhibition of Ras1 signaling leads to reduced *Appl* expression, whereas constitutive activation drives ectopic *Appl* expression. We show that *Appl* is directly regulated by the Ras/MAPK pathway through a mechanism mediated by PntP2, an ETS transcription factor that specifically binds ETS sites in the *Appl* regulatory region. We also found that zebrafish *appb* expression increased after ectopic *fgfr* activation in the neural tube of zebrafish embryos, suggesting a conserved regulatory mechanism.

Key words: Appl, ETS binding site, Axon targeting, Photoreceptor, Ras

Introduction

Differentiation of photoreceptors in the *Drosophila* compound eye requires activation of Ras1 and mitogen-activated protein kinase (MAPK) downstream of a receptor tyrosine kinase (RTK). In most photoreceptor precursors, Ras1/MAPK is activated by the RTK *Drosophila* Epidermal Growth Factor Receptor (DER) (Freeman, 1996). In the R7 photoreceptor precursor, however, the same Ras1/MAPK cassette is activated by an additional RTK, the Sevenless RTK (Sev) (Banerjee et al., 1987b; Hafen et al., 1987). Both RTKs are required for R7 determination, since significantly higher levels of Ras1/MAPK activation are necessary for R7 to overcome specific repressive mechanisms that would otherwise transform it into a non-neural cone cell. Sev is expressed in several photoreceptor precursors and in the four cone cells (Banerjee et al., 1987a; Tomlinson et al., 1987). However, only the presumptive R7 will activate the Sev receptor. Although the complex regulatory network involved in R7 specification has been extensively investigated, little is known about the genetic program that responds to these RTK signals.

Here, we explore the transcriptional profile downstream of Ras/MAPK-mediated Sev signaling and show that *β amyloid protein precursor-like* (*Appl*), the fly ortholog of the human β amyloid precursor protein (*APP*) (Hardy and Selkoe, 2002; Rosen et al., 1989) is a direct target of Ras1/MAPK required for R7 function. Appl belongs to the APP family, which is conserved across species from *Caenorhabditis elegans* to mammals (Daigle and Li, 1993; Rosen et al., 1989). In humans, APP is the precursor of the Aβ peptide, which is involved in the development of Alzheimer's disease. In addition to mutations in the coding region that favor cleavage to produce the Aβ-peptide, aberrant expression of *APP* has also been associated with Alzheimer's disease (AD) (Koo et al., 1990; Palmert et al., 1988). Remarkably, different ligands of membrane receptors with intrinsic tyrosine kinase activity modulate *APP* expression in mammalian cell cultures (Cosgaya et al., 1996; Lahiri and Nall, 1995; Ohyagi and Tabira, 1993; Ruiz-León and Pascual, 2001). Moreover, some *APP* regulatory sequences that respond to Ras/MAPK have been characterized in PC12 cells (Villa et al., 2001).

Despite some evidences in cultured cells, little is known about APP regulation in tissues and organs *in vivo*. Therefore, we decided to use *Drosophila* advanced genetic and genomic tools to analyze Ras/MAPK regulation of *Appl* expression. In flies, *Appl* is specifically expressed in postmitotic neurons at all stages of development (Martin-Morris and White, 1990) and has been implicated in axonal transport (Gunawardena and Goldstein, 2001; Torroja et al., 1999a), neuronal development (Li et al.,

Journal of Cell Science

2004; Merdes et al., 2004) synaptic bouton formation (Ashley et al., 2005; Torroja et al., 1999b) response to traumatic brain injury (Leyssen et al., 2005) and protection against neurodegeneration of processed *Appl* products (Wentzell et al., 2012). Furthermore, human APP rescues the behavioral phenotype of the *Drosophila Appl* loss-of-function mutant, indicating an evolutionarily conserved role (Luo et al., 1992). In this work we studied the function of *Appl* in the R7 and found that it is required for R7 targeting and light discrimination. In addition, it is not yet clear whether *Appl* as well as mammalian APP transcriptional activation responds to Ras1 or to neural differentiation. We took advantage of the *Drosophila* genetic tools to study Ras1-mediated activation of *Appl* at single cell resolution in the intact developing retina. Our study provides a description of the Ras1 transcriptional regulation of *Appl* and offers useful insights into the mechanisms by which RTKs and the Ras/MAPK pathway regulate the differentiation of a neural cell type. Furthermore, our findings may be of relevance to understanding the pathophysiology of human disorders such as Alzheimer's disease.

Results and Discussion

Analysis of the Sev-controlled transcriptome in R7 photoreceptors

To investigate the transcriptome controlled by Sev in the R7 photoreceptor, we analyzed microarrays using eye imaginal discs from third instar larvae in the *sev* mutants sev^{S11} and sev^{d2} compared with wild-type controls. The gain-of-function (GOF) allele sev^{S11} encodes a ligand-independent activated Sev receptor and generates flies with extra R7 photoreceptors, whereas the loss-of-function (LOF) allele sev^{d2} impairs the formation of R7 (Basler et al., 1991). The entire set of microarrays was normalized following the same protocol (see Materials and Methods). This kind of standardization allowed us to include a third computational comparison: sev^{s11} against sev^{d2} (GOF/LOF). The number of genes with significantly modified expression (1.5-fold change, and false-discovery-rate-corrected $P<0.05$) is shown in supplementary material Table S1 .

As Ras1 acts through the MAPK cascade to activate transcription (Plotnikov et al., 2011), we restricted the list of genes to those that were transcriptionally activated. We defined this population as target genes, which correspond to genes with increased expression in GOF/wild type or GOF/LOF, and those with decreased expression in LOF/wild type. The total number of genes obtained was 233. The functional annotation of target genes using Gene Ontology (GO) is shown in Fig. 1.

MAPK controls neural development through phosphorylation of the transcriptional repressor Yan and the transcriptional activator Pointed-P2 (PntP2) (Brunner et al., 1994). Both proteins are able to recognize ETS binding sites, DNA consensus sequences that are well characterized and conserved (Oikawa and Yamada, 2003). To restrict the list of target genes to those candidates directly regulated by the MAPK cascade, we performed a computational search for ETS binding sites in the upstream promoters (1000 bp upstream from the transcription start site) and introns of the target genes using the genomes of 12 Drosophilidae to strengthen the predictions (Clark et al., 2007). Thirty-eight genes with ETS binding sites were identified as ETS target genes (supplementary material Table S2). The GO annotation of these genes contained categories consistent with the molecular program activated by Ras1 in the R7 cell (Fig. 1B).

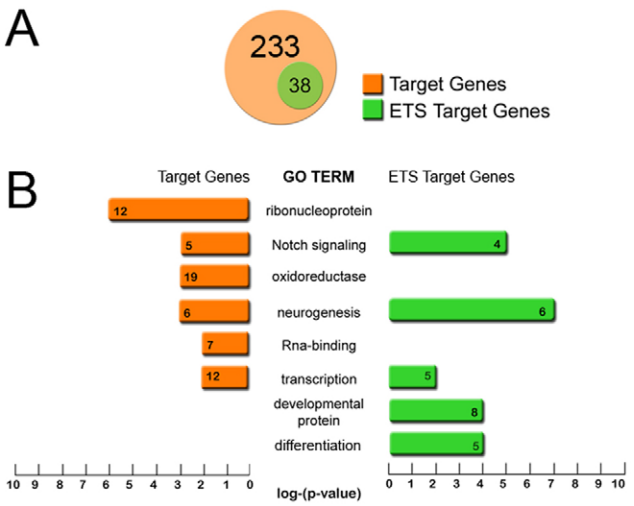

Fig. 1. Whole genome expression profiles of Sevenless. (**A**) Diagram showing the intersection between Sev target genes (orange) and ETS target genes (green). (**B**) Gene ontology (GO) terms of Sev target genes and ETS target genes. The number of genes in each category is shown within bars. The length of the bars indicates the fold change (enrichment in these transcriptomes compared to the whole genome, $P<0.05$ in all cases).

Appl was classified within the over-represented category 'neurogenesis' containing putative neural genes that respond to Ras1 in R7 neural precursors (supplementary material Table S2). Hereafter, we decided to focus on *Appl* regulation because of the biomedical implications.

Appl is differentially expressed in photoreceptor precursor cells

Appl mRNA was found in photoreceptors as they are recruited into developing clusters (Fig. 2A). It first appears in the precursor of R8, followed by R2/5, R3/4, R1/6, and finally R7 (Fig. 2A,B). It was undetectable in unspecified cells and cone cells (Fig. 2A,B), in agreement with previous studies (Luo et al., 1990; Torroja et al., 1996). Antibodies directed against the N-terminal ectodomain, show a punctuate distribution at the membrane of all photoreceptors and developing axons (Torroja et al., 1996). We re-examined the expression of Appl protein in the eye and observed differences in Appl distribution between photoreceptors. Confocal sagittal and horizontal sections of eye discs showed Appl to be predominantly expressed in R7 and R8 photoreceptors (Fig. 2B). This prevailing localization was more evident in the posterior part of the disc, where all cells are already specified. High levels of Appl in R7 correlate with the increased expression of *Appl* detected in *sev* GOF arrays. *Appl* upregulation by activated *Sev* was further confirmed by *in situ* hybridization and immunostaining of sev^{S11} eye discs (Fig. 2C,D). As shown in Fig. 2C, greater *Appl* mRNA accumulation was observed in sev^{S11} eye discs compared with wild-type discs, and higher levels of Appl protein were found in cells transformed to an R7 fate (compare Fig. 2B and 2D).

Function of Appl in the R7 photoreceptor

Next, we examined the relation between high *Appl* expression and R7 function. Adult flies normally display a phototactic response involving a preference for UV over visible light that relies on perception of UV light by the R7 photoreceptor (Harris

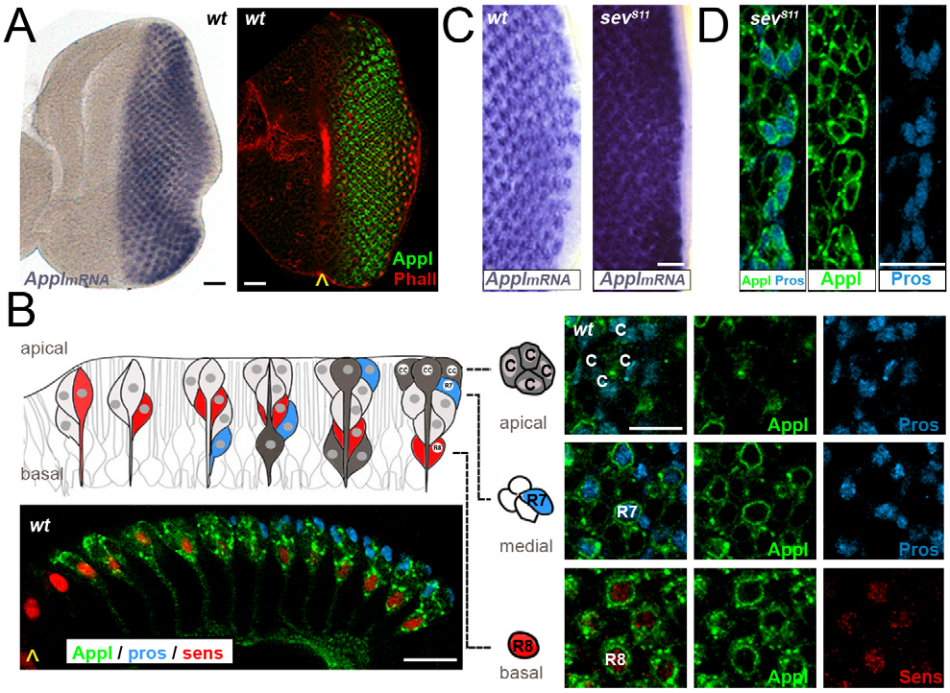

Fig. 2. *Appl* expression in the eye imaginal disc. (**A**) *In situ* hybridization for *Appl* mRNA and immunostaining for Appl in developing ommatidia just posterior to the morphogenetic furrow (yellow chevron in right panel), co-stained with phalloidin (red). (**B**) Drawing of a cross section of an eye imaginal disc showing the apico-basal organization of the epithelium (Wolff and Ready, 1993). From left to right, this cartoon depicts the progressive recruitment of photoreceptor precursors (R1–6, light gray; R7, blue; R8, red) and cone cells (cc, dark gray) into ommatidial clusters. The most mature ommatidia (right) already show the final cluster organization (apical, cone cells; medial, R1–R7; basal, R8). Confocal image below the cartoon: sagittal optical section of an eye disc, with the more mature clusters on the right side. Yellow chevron: the morphogenetic furrow; red: R8; blue: R7; green: Appl. Right images: three different planes of mature ommatidia after Appl immunostaining. Upper row: apical level showing cone cells stained with anti-prospero (blue) and absence of Appl (green). Middle row: R7 level, stained with anti-prospero. Appl is localized on the surface of the R7 and to at a much lower level on other photoreceptors (surrounding R7). Lower row: section through the R8 level also with high Appl localization (co-stained with anti-senseless). (**C**) *In situ* hybridization of *Appl* in wild-type and sev^{S11} eye discs. (**D**) Sev^{S11} discs have extra R7 photoreceptors in the ommatidia, and Appl immunostaining reveals expression in all the extra R7s (co-stained with anti-prospero). This image shows four ommatidia with extra R7s. In all images anterior is to the left. Scale bars: 10 μm.

et al., 1976). As a consequence, R7 function can be analyzed using a spectral-preference assay (see Materials and Methods). We used this assay to assess the functional role of Appl in R7 and found that flies carrying the null mutation $Appl^d$ exhibited reduced UV preference compared to wild-type flies (Fig. 3A). Since $Appl^d$ eyes contain all photoreceptors, including R7

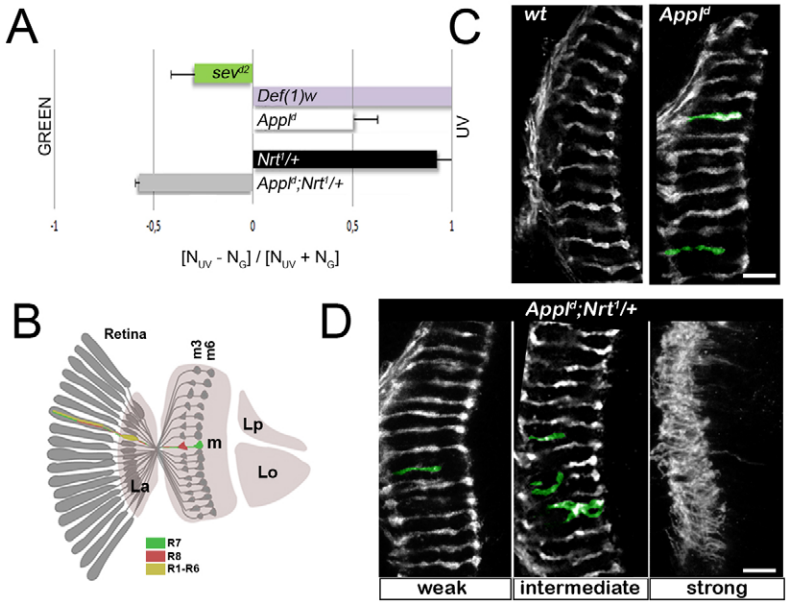

Fig. 3. Appl function in the R7 photoreceptor. (**A**) Spectral preference assay. The number of flies choosing UV (N_{UV}) or green (N_G) light was counted and used to calculate the choice index $[(N_{UV}-N_G)/(N_{UV}+N_G)]$. *Df(1)w* flies used as control tend to move towards UV light, whereas Sev^{d2} homozygous flies, which lack R7s, move towards green light. The preference of $Appl^d$ homozygous flies for UV light is much lower than controls. This phenotype is dramatically enhanced in combination with heterozygous Nrt^1. Note that Nrt^1 flies in heterozygosis behave similarly to *Df(1)w* flies. (**B**) Schematic representation of *Drosophila* photoreceptor cell projections from the adult retina into the lamina (La, R1–R6) and medulla (m, R8/R7) of the optic lobe; the more central optic ganglia [lobula (Lo) and lobula plate (Lp)] are shown. (**C**,**D**) Projection of R7 and R8 axons visualized with anti-chaoptin (mistargeted R7 photoreceptors are shown in green) in $Appl^d$ (C) and $Appl^d;Nrt^1/+$ (D) medullas. Scale bars: 10 μm.

(supplementary material Fig. S1A), *Appl* does not contribute to neural specification. We therefore assessed the possibility that *Appl* is involved in regulating R7 axonal targeting. Photoreceptor neurons establish synapses in the peripheral lamina and the deeper medulla of the optic lobe. The R8 and R7 neurons of each ommatidium project their axons into the same horizontal column of the medulla but synapse in different layers: M3 and M6, respectively (Ting and Lee, 2007) (Fig. 3B). R7 axons in $Appl^{d}$ flies were found to be mistargeted in 2% of the R7 photoreceptors examined (Fig. 3C). This lack of a severe phenotype in $Appl^{d}$ mutant eyes was not surprising, since several molecules are known to be involved in axonal targeting (Hadjieconomou et al., 2011). Thus, other transmembrane proteins might mask the $Appl^{d}$ phenotype. To address this possibility, we sensitized $Appl^{d}$ flies using different genetic backgrounds in heterozygosis for other alleles of membrane proteins *frazzled* (fra^{3}) (Kolodziej et al., 1996), *fasciclinIII* ($fasIII^{E25}$) (Chiba et al., 1995), *NCadherin* ($CadN^{m19}$) (Iwai et al., 1997) and *neurotactin* (Nrt^{1}) (Speicher et al., 1998) and tested them alone and in combination with $Appl^{d}$ in the spectral preference assay. We found that $Appl^{d}$ flies carrying any of those mutant alleles had a greater frequency of incorrect response to UV light (supplementary material Fig. S1B). The strongest phenotype was observed in the combination of $Appl^{d}$ with axon guidance protein *neurotactin* (*Nrt*) (Fig. 3A), which confirms their genetic interaction (Merdes et al., 2004). These data suggest that Appl appears to cooperate with multiple guidance receptors for correct R7 targeting. We therefore analyzed the targeting of R7 to the M6 layer in $Appl^{d}/Appl^{d};Nrt^{1}/+$ flies. We recovered phenotypes with differences in severity that can be divided into three categories: (1) weak phenotype (56% of brains) that resembles that of $Appl^{d}$ mutants with 3% of mistargeted R7; (2) intermediate (30%) phenotype with 12.5% of mistargeted R7; and (3) strong (14%) phenotype in which the axons are completely disorganized ($n=14$; Fig. 3D). These findings further support a role for Appl in R7 axon targeting and suggest a function for Appl in R7-mediated discrimination of UV light.

Ras1 signaling is required for *Appl* expression

To evaluate whether Ras1 signaling is required for *Appl* expression we generated clones of mutant alleles that interfere with or enhance Ras1 pathway activity. We first induced clones expressing a dominant-negative form of *DER* (DER^{DN}). These clones caused complete loss of *Appl* expression (Fig. 4A), indicating that DER is required for *Appl* expression. We next analyzed clones expressing the constitutively active form of *Ras1*, Ras^{V12}. We observed that expression of Ras^{V12} is sufficient to cell-autonomously activate *Appl* in the eye (Fig. 4B). Ras1 activity can induce photoreceptor differentiation, whereas DER^{DN} prevents photoreceptor formation (Freeman, 1996; Spencer et al., 1998). Therefore, to clarify whether *Appl* expression is downstream of Ras1 signaling or alternatively an indirect consequence of photoreceptor specification, we analyzed the R8 precursor, which does not require Sev and DER for its specification (Yang and Baker, 2001) We generated clones carrying a null allele of *Ras1* ($Ras1^{\Delta C40b}$) near the morphogenetic furrow that precedes photoreceptor differentiation and then examined the zinc finger protein encoded by *senseless*, which is a specific marker of the R8 precursor. We found that *Appl* expression was severely reduced or absent in those clones (Fig. 4C), indicating that Ras1 controls its expression independently of photoreceptor specification.

The transcriptional activator PntP2 mediates Ras1/MAPK activation of *Appl*

The transcriptional output of the canonical Ras1/MAPK pathway is usually mediated by the transcription factor *PntP2* (Brunner et al., 1994; O'Neill et al., 1994). To assess whether *PntP2* mediates Ras1/MAPK activation of *Appl*, we generated twin clones of the loss-of-function allele $pnt^{\Delta 88}$. In these clones, we observed R8 cells with severely reduced Appl expression (Fig. 4D) that strongly resembled the expression in *Ras1* loss-of-function clones. This result indicates that PntP2 mediates Ras1/MAPK activation of *Appl* expression and is consistent with a putative direct regulation of *Appl* through PntP2 binding to specific ETS regulatory sequences.

Consistent with a proposed role of ETS binding sites, we found four conserved ETS predictions distributed in two *Appl* introns (ETS1and ETS4; Fig. 4E; supplementary material Fig. S2). To evaluate whether PntP2 is able to induce gene expression through binding to *Appl* ETS sites, we generated enhancer-*lacZ* reporters for all four ETS sites in flies and found that Ras^{v12} is sufficient to activate ETS1 and 3, when ectopically expressed in clones (supplementary material Fig. S3). None of the constructs produced endogenous β-galactosidase expression in wild-type eye discs. This may be because the binding sites for other transcriptional regulators that cooperate with the endogenous expression are missing in this construct. Nevertheless, to validate PntP2 binding, we performed chromatin immunoprecipitation (ChIP) assays with eye imaginal discs. Owing to the lack of antibodies against PntP2, we generated a transgenic fly carrying a HA-tagged *PntP2* under the UAS inducible promoter (supplementary material Fig. S4A). The *UAS-PntP2-HA* transgene under a *sev-Gal4* driver restricts expression to the Sev-expressing cells of the eye (R1/6, R3/4, R7, and cone cells). To enhance PntP2 activity, we performed the experiment in a sev^{S11} background (supplementary material Fig. S4B). Subsequently, we performed ChIP-PCR experiments with those imaginal discs expressing PntP2-HA using an anti-HA antibody (Fig. 4F,G). To assess the antibody background, we also performed ChIP on wild-type discs lacking PntP2-HA (Fig. 4G). Our results showed an enrichment of the *Appl* ETS1 site bound to PntP2, whereas no enrichment was observed for the *Appl* ETS2 site (Fig. 4G). This result demonstrates that *Appl* is a direct target of Ras1/MAPK signaling through direct binding of PntP2 to *Appl* ETS1.

Our results raise the question of whether RTK signaling could also regulate expression of the APP family in vertebrates. Ligands of RTKs such as NGF, FGF and EGF increase *APP* mRNA levels in mammalian cell lines (Cosgaya et al., 1996; Ruiz-León and Pascual, 2001). Since most of these observations have been performed in cell culture, we used an alternative vertebrate developmental system to test *APP* transcriptional regulation by RTKs *in vivo*. We analyzed activation of *appb*, a fish ortholog of *Appl*, in a zebrafish transgenic line, which expresses a constitutively active form of the *Xenopus* Fibroblast Growth Factor Receptor 1 (*fgfr1*) in response to heat shock. *Appb* is expressed in the early developing central nervous system including the retina (Lee and Cole, 2007; Musa et al., 2001). Heat-shock treatment of *ca-fgfr1* transgenic embryos resulted in a dramatic increase of *appb* compared to control embryos

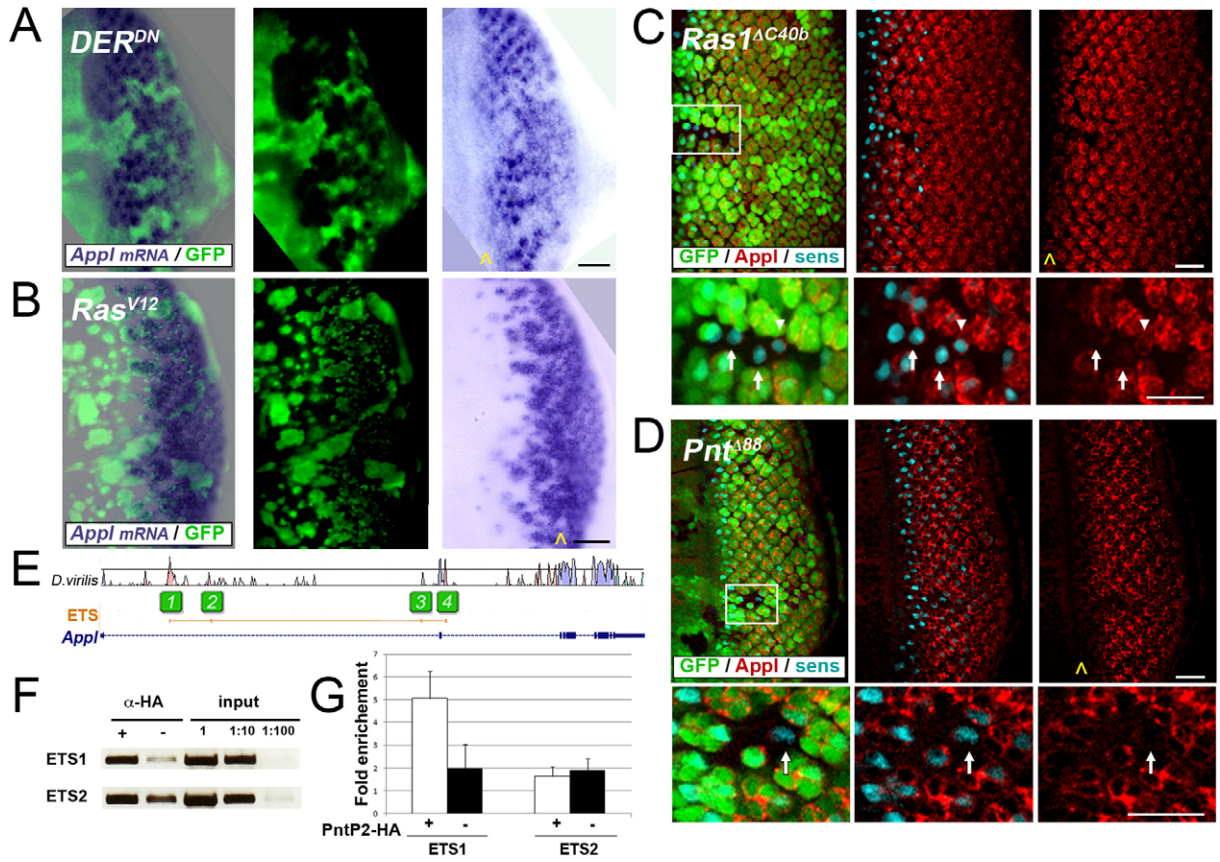

Fig. 4. Appl expression is regulated by Ras1/MAPK. (**A**) *In situ* hybridization for *Appl* in clones expressing DER^{DN} (GFP) reveals absence of *Appl* mRNA. (**B**) Clones expressing Ras^{V12} (GFP) have ectopic *Appl* mRNA anterior to the morphogenetic furrow (yellow chevron), where *Appl* is normally not expressed. (**C**,**D**) Homozygous mutant clones (lack of GFP) in heterozygous tissues. Lower panels: detail of regions indicated by white squares. R8 cells labeled with anti-senseless antibody (cyan) in $Ras1^{\Delta C40b}$ (C) and $Pnt^{\Delta 88}$ (D) clones near to the morphogenetic furrow (yellow chevron) show reduction (arrowhead) or absence (arrows) of Appl protein. In all images, anterior is to the left. Scale bars: 10 µm. (**E**) Graphical representation of *Appl* ETS sites (1–4) and VISTA comparison between Appl genes of *Drosophila melanogaster* and *Drosophila virilis*. (**F**) ChIP-PCR of eye imaginal discs expressing PntP2-HA immunoprecipitated with anti-HA antibody (+). As a negative control, an aliquot was immunoprecipitated without antibody (−). Non-immunoprecipitated chromatin was used as the input sample. Regions of ~500 bp spanning ETS1 and ETS2 were amplified by PCR. (**G**) Quantification of ChIP-PCRs from eye imaginal discs expressing PntP2-HA (+; n=3 replicates), and wild-type discs lacking PntP2-HA (−; n=2 replicates) normalized to the negative control (an aliquot immunoprecipitated without antibody) and depicted as fold enrichment for ETS1 and ETS2.

(supplementary material Fig. S5). This finding suggests an evolutionarily conserved mechanism of *appb* regulation by RTK. Further experiments will help to clarify whether deregulated RTK/Ras1 is implicated in the progression of neurodegeneration and aberrant accumulation of APP in pathological conditions.

In summary, two main conclusions can be drawn from this work. First, *Drosophila Appl* is involved in R7 axonal targeting. Moreover, our finding that the *Appl* loss-of-function defects are enhanced when combined with *Nrt* heterozygous mutant suggest that Appl acts at the membrane of R7, where it interacts with other proteins such as Nrt. Second, *Appl* activation downstream of the RTK/Ras1 is independent of neural specification, occurs in vivo, and is mediated by direct binding of PntP2 to ETS sequences in the *Appl* regulatory region.

Together, these findings may provide insights into the pathogenesis of neurological disorders such as Alzheimer's disease. The β-amyloid peptides, which accumulate in the amyloid plaques found in the brain of Alzheimer's disease patients, are produced after APP proteolysis. However, Alzheimer's disease has not only been associated to the production of the primary component Aβ by proteolysis of APP, but also by transcriptional regulation. Increased *APP* transcription underlies the phenotype in some cases of familial Alzheimer's disease (Querfurth et al., 1995). In addition, overexpression of *APP* appears to be responsible for the early onset of Alzheimer's disease in individuals with Down syndrome (Rumble et al., 1989). Thus, our results open the possibility to explore whether in some cases of Alzheimer's disease a burst of RTK/Ras1/MAPK occurs and whether this signaling activity ends with high APP accumulation.

Amyloid β peptides are known to be involved in vision dysfunction caused by age-related retinal degeneration in mouse models (Ding et al., 2008; Ning et al., 2008). Thus, our *in vivo* observations could be the basis for further research in mammalian models for neurodegenerative retinal disorders that share several pathological features with Alzheimer's disease.

Materials and Methods

Fly strains, transgenes and clonal analysis

Alleles used in this work: Sev^{s11} and $sev\text{-}Gal4sev^{S11}$ (Basler et al., 1991); sev^{d2} (Gerresheim, 1988); $UAS\text{-}DER^{DN}$ (Freeman, 1996; Scholz et al., 1997); $UAS\text{-}Ras^{V12}$

(Scholz et al., 1997); *Ras1*$^{\Delta C40b}$ (Hou et al., 1995); *Pnt*$^{\Delta 88}$ (Scholz et al., 1993); *fra*^{3} (Kolodziej et al., 1996); *fas3*^{E25} (Snow et al., 1989); *CadN*^{m19} (Iwai et al., 1997); *Nrt*^{1} (Hortsch et al., 1990); *Df(1)w* and *Appl*^{d} (Luo et al., 1992). To generate *UAS-PntP2* transgenic flies, full-length *Pnt-RB* and three copies of the HA epitope were cloned between the *Xho*I and *Xba*I sites of the pUASTattB vector and inserted in the 68E site of integrase trangenesis system. *ETS1·LacZ*, *ETS2·LacZ*, *ETS3·LacZ*, and *ETS4·LacZ* transgenic flies were generated by cloning *Appl* genomic fragments that encompass the ETS predictions and surrounding nucleotides with high conservation scores across 12 *Drosophila* genomes, to avoid introduction of a potentially fragmenting enhancer. Fragments of ~500 bp were cloned in the pLacZattB vector (http://flyc31.frontiers-in-genetics.org/sequences_and_vectors.php) upstream of the Hsp70 minimal promoter driving nuclear *lacZ* and inserted into a predefined genomic position 86Fb via ΦC31-mediated transgenesis.

Clones overexpressing UAS transgenes were induced by a 10-minute heat shock at 37℃ to activate the hsFlp. Clones of homozygous mutant cells were induced by incubation at 37℃ for 45 minutes. Clones were generated at 60 hours after egg laying. In all cases eye discs were analyzed at 120 hours after egg laying. Genotypes used for clonal analysis with FRTs in cis: *w,hsFlp;Act FRT y+FRTGal4::UAS-GFP* were used to drive the following transgenes: *UAS-Ras*^{V12} or *UAS-DER*^{DN}. For clonal analysis of FRTs in trans: *w, hsFlp; FRT82B UbiGFP* and *FRT82B Ras1*$^{\Delta C40b}$ or *FRT82B pnt*^{A88}.

Microarray analyses

Two-color microarray design and analyses were carried out as previously reported (Beltran et al., 2007; Blanco et al., 2010). Total RNA was extracted from eye-antenna imaginal discs from wandering blue-gut staged early third instar larvae using the RNeasy Protect Mini Kit (Qiagen Inc., Valencia, CA, USA). At least two independent total RNA extractions were carried out from sev^{S11} and sev^{d2} strains. Total RNA from *w*^{1118} was used as a common reference. We obtained lists of genes that were differentially expressed (had an FDR-corrected $P<0.05$ and at least two spots from the four replicate arrays that passed the quality filters) over 1.5- or 2.0-fold in the mutants compared to the reference strain. Raw and normalized data are deposited in the Gene Expression Omnibus (GEO) database [http://www.ncbi.nlm.nih.gov/projects/geo/] with the accession number GSE37793.

Promoter and intron characterization

We extracted 1000 nucleotides upstream of the transcription start site and the intron sequences of our set of 233 target genes, according to RefSeq annotations in the University of California, Santa Cruz (UCSC) genome browser. We used the MatScan program (Blanco et al., 2006) to analyze these sequences with Jaspar and Transfac predictive models for ETS. We converted these predictions into the UCSC custom track format to map them along the *D. melanogaster* genome. Using the Conservation track (multiple alignment of *Drosophila* species), we filtered out the predictions that were not conserved in at least five species (including *D. pseudoobscura* or more distant species).

Immunohistochemistry

Adult brains (1 to 3 days old) and eye imaginal discs where processed for antibody staining using conventional techniques. Primary antibodies: anti-GFP rabbit serum (1:1000, Santa Cruz Biotechnology, Inc., Santa Cruz, CA), rabbit anti-β-galactosidase (1:1000, Cappel, ICN/Cappel, Aurora, OH), mouse anti-Prospero, mouse anti-Elav and mouse anti-Chaoptin (1:20, 1:100 and 1:10, respectively) from Developmental Studies Hybridoma Bank (Iowa City, IA), guinea pig anti-senseless (1:800; H. Bellen, Baylor College of Medicine, Houston, USA), Rabbit anti-Appl (1:1600, L. Torroja, Universidad Autónoma de Madrid, Spain), Rhodamine phalloidin (1:40, Molecular Probes, Invitrogen). Images were obtained with a Leica SPE confocal microscope and processed with ImageJ and Adobe Photoshop 7.0 software.

In situ hybridization

In situ hybridization was carried out on eye imaginal discs fixed with 4% formaldehyde using digoxigenin-labeled antisense RNA probes according to standard protocols. Riboprobes for *Appl* were synthesized using a cDNA clone from DGC (GH04413), sequenced using primers from the SP6 and T7 promoters and linearized with *Eco*RI for antisense probe. Discs were then analyzed with a Leica DMLB fluorescence microscope. In experiments using Flp/Gal4 clones, anti-digoxigenin and anti-GFP incubations were done simultaneously. Secondary antibody incubation was performed after color development with NBT/BCIP.

Zebrafish *in situ* hybridization and overexpression of ca-fgfr1

Whole-mount *in situ* hybridization using digoxigenin-labeled antisense RNA probes was carried out using standard protocols. Riboprobes for *Appb* were synthesized from cDNA of embryos at 6 days post-fertilization. The Tg(hsp70:ca-fgfr1) transgenic line (Marques et al., 2008) was used to overexpress a constitutively active form of the *Xenopus* fgfr1 by applying a heat shock at 39℃ for 1 hour.

UV/green spectral preference

The UV/green spectral preference was carried out using a T-maze. Two arms of the T-maze were illuminated with either UV or green LEDs (370 nm from Optosource and 525 nm from Ledman Optoelectronic). Light intensity was calibrated such that control flies preferred the UV side. Flies were kept in darkness for 24 hours and then pre-adapted to white light for 1 hour before testing. They were then locked into a small compartment in the T-maze. Subsequently, the flies were allowed to enter the vials illuminated by either test light for 30 seconds. After each test, the flies in each vial were counted and the Choice Index (CI) calculated from the numbers choosing UV (N_{UV}) or green (N_G) light by the following formula: $CI=(N_{UV}-N_G)/(N_{UV}+N_G)$. The few flies remaining in the center compartment were discarded. For each genotype, three trials (~30 3- to 5-day-old flies per trial) were carried out. All genotypes for the heterozygous combinations were kept in a *Df(1)w* background. Flies *Df(1)w* are viable in homozygosis, carry the w^- and y^- markers and were used as controls for behavioral studies (Luo et al., 1992).

ChIP assay

Detailed procedure has been described before (Perez-Lluch et al., 2011). Third-instar larva eye imaginal discs isolated from *w; sev*^{S11}*sev-GAL4/UAS-PntP2-HA* were immunoprecipitated with anti-HA; three independent replicates were performed. As controls we used two independent replicates for discs lacking PntP2-HA. For PCRs, 2 µl of a 50 µl DNA extraction was amplified with specific primers. PCR bands were quantified using Fujifilm MultiGauge software, normalized against the negative control and depicted as fold enrichment. Specific primers: ETS1 FW 5′-TTCTTCTGACCCACTGCTC-3′, ETS1 RV 5′-GATGAGGGTACGCTGGTAG-3′, ETS2 FW 5′-CCGAGTGTGTGAGCGTG-AG-3′, ETS2 RV 5′-AAGCTCTGGACTACGAATGG-3′. The histograms in Fig. 4G represent the mean of the replicates. Standard error of the mean was applied for each experiment.

Acknowledgements

We thank G. Jimenez, L. Torroja, S. Araujo, S. Pérez, M. Morey and H. Bellen for reagents and discussions, and A. Mateo for technical support. We thank S. Beltran and A. Sànchez for their help with microarray analysis. We thank B. Hassan for insightful suggestions. We also thank the *Drosophila* Transformation and Bioinformatics (E. Blanco) Platforms of The Consolider Project.

Funding

This work was supported by an FPU grant of the Ministerio de Educación y Ciencia, Spain to N.M.; and by the Ministerio de Ciencia e Innovación [grant numbers BFU2009-09781 and CSD2007-00008 to F.S.].

Supplementary material available online at
http://jcs.biologists.org/lookup/suppl/doi:10.1242/jcs.114785/-/DC1

References

Ashley, J., Packard, M., Ataman, B. and Budnik, V. (2005). Fasciclin II signals new synapse formation through amyloid precursor protein and the scaffolding protein dX11/Mint. *J. Neurosci.* **25**, 5943-5955.

Banerjee, U., Renfranz, P. J., Hinton, D. R., Rabin, B. A. and Benzer, S. (1987a). The sevenless+ protein is expressed apically in cell membranes of developing Drosophila retina; it is not restricted to cell R7. *Cell* **51**, 151-158.

Banerjee, U., Renfranz, P. J., Pollock, J. A. and Benzer, S. (1987b). Molecular characterization and expression of sevenless, a gene involved in neuronal pattern formation in the Drosophila eye. *Cell* **49**, 281-291.

Basler, K., Christen, B. and Hafen, E. (1991). Ligand-independent activation of the sevenless receptor tyrosine kinase changes the fate of cells in the developing Drosophila eye. *Cell* **64**, 1069-1081.

Beltran, S., Angulo, M., Pignatelli, M., Serras, F. and Corominas, M. (2007). Functional dissection of the ash2 and ash1 transcriptomes provides insights into the transcriptional basis of wing phenotypes and reveals conserved protein interactions. *Genome Biol.* **8**, R67.

Blanco, E., Messeguer, X., Smith, T. F. and Guigó, R. (2006). Transcription factor map alignment of promoter regions. *PLoS Comput. Biol.* **2**, e49.

Blanco, E., Ruiz-Romero, M., Beltran, S., Bosch, M., Punset, A., Serras, F. and Corominas, M. (2010). Gene expression following induction of regeneration in Drosophila wing imaginal discs. Expression profile of regenerating wing discs. *BMC Dev. Biol.* **10**, 94.

Brunner, D., Dücker, K., Oellers, N., Hafen, E., Scholz, H. and Klämbt, C. (1994). The ETS domain protein pointed-P2 is a target of MAP kinase in the sevenless signal transduction pathway. *Nature* **370**, 386-389.

Chiba, A., Snow, P., Keshishian, H. and Hotta, Y. (1995). Fasciclin III as a synaptic target recognition molecule in Drosophila. *Nature* **374**, 166-168.

Clark, A. G., Eisen, M. B., Smith, D. R., Bergman, C. M., Oliver, B., Markow, T. A., Kaufman, T. C., Kellis, M., Gelbart, W., Iyer, V. N. et al.; DROSOPHILA 12 GENOMES CONSORTIUM (2007). Evolution of genes and genomes on the Drosophila phylogeny. *Nature* **450**, 203-218.

Cosgaya, J. M., Latasa, M. J. and Pascual, A. (1996). Nerve growth factor and ras regulate beta-amyloid precursor protein gene expression in PC12 cells. *J. Neurochem.* **67**, 98-104.

Daigle, I. and Li, C. (1993). apl-1, a Caenorhabditis elegans gene encoding a protein related to the human beta-amyloid protein precursor. *Proc. Natl. Acad. Sci. USA* **90**, 12045-12049.

Ding, J. D., Lin, J., Mace, B. E., Herrmann, R., Sullivan, P. and Bowes Rickman, C. (2008). Targeting age-related macular degeneration with Alzheimer's disease based immunotherapies: anti-amyloid-beta antibody attenuates pathologies in an age-related macular degeneration mouse model. *Vision Res.* **48**, 339-345.

Freeman, M. (1996). Reiterative use of the EGF receptor triggers differentiation of all cell types in the Drosophila eye. *Cell* **87**, 651-660.

Gerresheim, F. (1988). Isolation of Drosophila melanogaster mutants with a wavelength-specific alteration in their phototactic response. *Behav. Genet.* **18**, 227-246.

Gunawardena, S. and Goldstein, L. S. (2001). Disruption of axonal transport and neuronal viability by amyloid precursor protein mutations in Drosophila. *Neuron* **32**, 389-401.

Hadjieconomou, D., Timofeev, K. and Salecker, I. (2011). A step-by-step guide to visual circuit assembly in Drosophila. *Curr. Opin. Neurobiol.* **21**, 76-84.

Hafen, E., Basler, K., Edstroem, J. E. and Rubin, G. M. (1987). Sevenless, a cell-specific homeotic gene of Drosophila, encodes a putative transmembrane receptor with a tyrosine kinase domain. *Science* **236**, 55-63.

Hardy, J. and Selkoe, D. J. (2002). The amyloid hypothesis of Alzheimer's disease: progress and problems on the road to therapeutics. *Science* **297**, 353-356.

Harris, W. A., Stark, W. S. and Walker, J. A. (1976). Genetic dissection of the photoreceptor system in the compound eye of Drosophila melanogaster. *J. Physiol.* **256**, 415-439.

Hortsch, M., Patel, N. H., Bieber, A. J., Traquina, Z. R. and Goodman, C. S. (1990). Drosophila neurotactin, a surface glycoprotein with homology to serine esterases, is dynamically expressed during embryogenesis. *Development* **110**, 1327-1340.

Hou, X. S., Chou, T. B., Melnick, M. B. and Perrimon, N. (1995). The torso receptor tyrosine kinase can activate raf in a ras-independent pathway. *Cell*, **81** 63-71.

Iwai, Y., Usui, T., Hirano, S., Steward, R., Takeichi, M. and Uemura, T. (1997). Axon patterning requires DN-cadherin, a novel neuronal adhesion receptor, in the Drosophila embryonic CNS. *Neuron* **19**, 77-89.

Kolodziej, P. A., Timpe, L. C., Mitchell, K. J., Fried, S. R., Goodman, C. S., Jan, L. Y. and Jan, Y. N. (1996). frazzled encodes a Drosophila member of the DCC immunoglobulin subfamily and is required for CNS and motor axon guidance. *Cell* **87**, 197-204.

Koo, E. H., Sisodia, S. S., Cork, L. C., Unterbeck, A., Bayney, R. M. and Price, D. L. (1990). Differential expression of amyloid precursor protein mRNAs in cases of Alzheimer's disease and in aged nonhuman primates. *Neuron* **4**, 97-104.

Lahiri, D. K. and Nall, C. (1995). Promoter activity of the gene encoding the beta-amyloid precursor protein is up-regulated by growth factors, phorbol ester, retinoic acid and interleukin-1. *Brain Res. Mol. Brain Res.* **32**, 233-240.

Lee, J. A. and Cole, G. J. (2007). Generation of transgenic zebrafish expressing green fluorescent protein under control of zebrafish amyloid precursor protein gene regulatory elements. *Zebrafish* **4**, 277-286.

Leyssen, M., Ayaz, D., Hébert, S. S., Reeve, S., De Strooper, B. and Hassan, B. A. (2005). Amyloid precursor protein promotes post-developmental neurite arborization in the Drosophila brain. *EMBO J.* **24**, 2944-2955.

Li, Y., Liu, T., Peng, Y., Yuan, C. and Guo, A. (2004). Specific functions of Drosophila amyloid precursor-like protein in the development of nervous system and nonneural tissues. *J. Neurobiol.* **61**, 343-358.

Luo, L. Q., Martin-Morris, L. E. and White, K. (1990). Identification, secretion, and neural expression of APPL, a Drosophila protein similar to human amyloid protein precursor. *J. Neurosci.* **10**, 3849-3861.

Luo, L., Tully, T. and White, K. (1992). Human amyloid precursor protein ameliorates behavioral deficit of flies deleted for Appl gene. *Neuron* **9**, 595-605.

Marques, S. R., Lee, Y., Poss, K. D. and Yelon, D. (2008). Reiterative roles for FGF signaling in the establishment of size and proportion of the zebrafish heart. *Dev. Biol.* **321**, 397-406.

Martin-Morris, L. E. and White, K. (1990). The Drosophila transcript encoded by the beta-amyloid protein precursor-like gene is restricted to the nervous system. *Development* **110**, 185-195.

Merdes, G., Soba, P., Loewer, A., Bilic, M. V., Beyreuther, K. and Paro, R. (2004). Interference of human and Drosophila APP and APP-like proteins with PNS development in Drosophila. *EMBO J.* **23**, 4082-4095.

Musa, A., Lehrach, H. and Russo, V. A. (2001). Distinct expression patterns of two zebrafish homologues of the human APP gene during embryonic development. *Dev. Genes Evol.* **211**, 563-567.

Ning, A., Cui, J., To, E., Ashe, K. H. and Matsubara, J. (2008). Amyloid-beta deposits lead to retinal degeneration in a mouse model of Alzheimer disease. *Invest. Ophthalmol. Vis. Sci.* **49**, 5136-5143.

O'Neill, E. M., Rebay, I., Tjian, R. and Rubin, G. M. (1994). The activities of two Ets-related transcription factors required for Drosophila eye development are modulated by the Ras/MAPK pathway. *Cell* **78**, 137-147.

Ohyagi, Y. and Tabira, T. (1993). Effect of growth factors and cytokines on expression of amyloid beta protein precursor mRNAs in cultured neural cells. *Brain Res. Mol. Brain Res.* **18**, 127-132.

Oikawa, T. and Yamada, T. (2003). Molecular biology of the Ets family of transcription factors. *Gene* **303**, 11-34.

Palmert, M. R., Golde, T. E., Cohen, M. L., Kovacs, D. M., Tanzi, R. E., Gusella, J. F., Usiak, M. F., Younkin, L. H. and Younkin, S. G. (1988). Amyloid protein precursor messenger RNAs: differential expression in Alzheimer's disease. *Science* **241**, 1080-1084.

Perez-Lluch, S., Blanco, E., Carbonell, A., Raha, D., Snyder, M., Serras, F. and Corominas, M. (2011). Genome-wide chromatin occupancy analysis reveals a role for ASH2 in transcriptional pausing. *Nucleic Acids Res.* **39**, 4628-4639.

Plotnikov, A., Zehorai, E., Procaccia, S. and Seger, R. (2011). The MAPK cascades: signaling components, nuclear roles and mechanisms of nuclear translocation. *Biochim. Biophys. Acta.* **1813**, 1619-1633.

Querfurth, H. W., Wijsman, E. M., St George-Hyslop, P. H. and Selkoe, D. J. (1995). Beta APP mRNA transcription is increased in cultured fibroblasts from the familial Alzheimer's disease-1 family. *Brain Res. Mol. Brain Res.* **28**, 319-337.

Rosen, D. R., Martin-Morris, L., Luo, L. Q. and White, K. (1989). A Drosophila gene encoding a protein resembling the human beta-amyloid protein precursor. *Proc. Natl. Acad. Sci. USA* **86**, 2478-2482.

Ruiz-León, Y. and Pascual, A. (2001). Brain-derived neurotrophic factor stimulates beta-amyloid gene promoter activity by a Ras-dependent/AP-1-independent mechanism in SH-SY5Y neuroblastoma cells. *J. Neurochem.* **79**, 278-285.

Rumble, B., Retallack, R., Hilbich, C., Simms, G., Multhaup, G., Martins, R., Hockey, A., Montgomery, P., Beyreuther, K. and Masters, C. L. (1989). Amyloid A4 protein and its precursor in down's syndrome and alzheimer's disease. *N. Engl. J. Med.* **320**, 1446-1452.

Scholz, H., Deatrick, J., Klaes, A. and Klämbt, C. (1993). Genetic dissection of pointed, a Drosophila gene encoding two ETS-related proteins. *Genetics* **135**, 455-468.

Scholz, H., Sadlowski, E., Klaes, A. and Klämbt, C. (1997). Control of midline glia development in the embryonic Drosophila CNS. *Mech. Dev.* **62**, 79-91.

Snow, P. M., Bieber, A. J. and Goodman, C. S. (1989). Fasciclin III: a novel homophilic adhesion molecule in Drosophila. *Cell* **59**, 313-323.

Speicher, S., García-Alonso, L., Carmena, A., Martín-Bermudo, M. D., de la Escalera, S. and Jiménez, F. (1998). Neurotactin functions in concert with other identified CAMs in growth cone guidance in Drosophila. *Neuron* **20**, 221-233.

Spencer, S. A., Powell, P. A., Miller, D. T. and Cagan, R. L. (1998). Regulation of EGF receptor signaling establishes pattern across the developing Drosophila retina. *Development* **125**, 4777-4790.

Ting, C. Y. and Lee, C. H. (2007). Visual circuit development in Drosophila. *Curr. Opin. Neurobiol.* **17**, 65-72.

Tomlinson, A., Bowtell, D. D., Hafen, E. and Rubin, G. M. (1987). Localization of the sevenless protein, a putative receptor for positional information, in the eye imaginal disc of Drosophila. *Cell* **51**, 143-150.

Torroja, L., Luo, L. and White, K. (1996). APPL, the Drosophila member of the APP-family, exhibits differential trafficking and processing in CNS neurons. *J. Neurosci.* **16**, 4638-4650.

Torroja, L., Chu, H., Kotovsky, I. and White, K. (1999a). Neuronal overexpression of APPL, the Drosophila homologue of the amyloid precursor protein (APP), disrupts axonal transport. *Curr. Biol.* **9**, 489-492.

Torroja, L., Packard, M., Gorczyca, M., White, K. and Budnik, V. (1999b). The Drosophila beta-amyloid precursor protein homolog promotes synapse differentiation at the neuromuscular junction. *J. Neurosci.* **19**, 7793-7803.

Villa, A., Latasa, M. J. and Pascual, A. (2001). Nerve growth factor modulates the expression and secretion of beta-amyloid precursor protein through different mechanisms in PC12 cells. *J. Neurochem.* **77**, 1077-1084.

Wentzell, J. S., Bolkan, B. J., Carmine-Simmen, K., Swanson, T. L., Musashe, D. T. and Kretzschmar, D. (2012). Amyloid precursor proteins are protective in Drosophila models of progressive neurodegeneration. *Neurobiol. Dis.* **46**, 78-87.

Wolff, T. and Ready, D. F. (1993). Pattern formation in the Drosophila retina. In *The Development of Drosophila melanogaster* (ed. M. Bate and A. Martinez Arias), pp. 1277-1326. New York, NY: Cold Spring Harbor Laboratory Press.

Yang, L. and Baker, N. E. (2001). Role of the EGFR/Ras/Raf pathway in specification of photoreceptor cells in the Drosophila retina. *Development* **128**, 1183-1191.